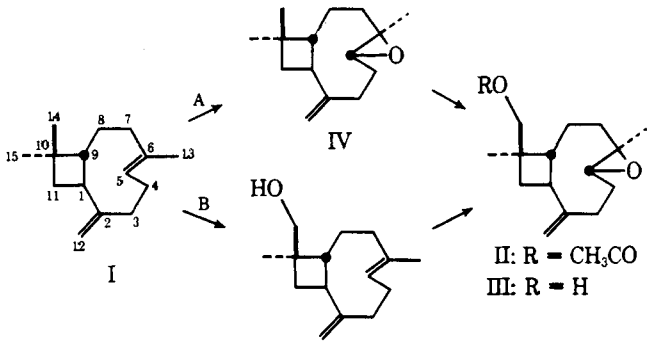

Scheme I

(each s, 3H), 2.92 (m, 1H, O–C–H), 3.55 (bs, 2H, CH_2OH), and 4.87 and 5.00 (each bs, 1H); 3450 cm^{-1} (OH). These results showed that the metabolic product and its acetate were represented best as III and II, respectively. The absolute configuration of the metabolized methyl group on a four-membered ring of I was established by X-ray study of II: [a = 9.624(4) Å, b = 8.599(4) Å, c = 10.214(4) Å, β = 105.47(3)°, space group $P2_1$, Dc = 1.13 g/cm^3, and z = 2]. The diffraction intensities were collected in the ω-scan mode, using graphite monochromated MoKα radiation on a diffractomer[2], and corrected for Lorenz polarization and background effects. The structure was resolved by direct methods using a Multan program (2) and was refined by full matrix least-squares calculations. The final R value was 0.092 for 1008 reflections. The relative stereostructure of II is shown in Fig. 1.

Two metabolic pathways may be present in the biotransformation of I (Scheme I). In this connection, (−)-caryophyllene oxide (IV), $[\alpha]_D$ −35.2° (*c*, 2.19 in chloroform), also was administered to rabbits by the method already described. After being acetylated, II was obtained as the major product from the neutral metabolites. Thus, route A was confirmed. Although the presence of route B remains to be clarified, route A may be more favorable than B since IV was found in some essential oils (3–5). According to biotransformation, the hydroxylation of the *gem*-dimethyl group on the three-, four-, five-, and six-membered rings was established for 3-carene (6, 7) and carane (7); caryophyllene; camphor (8) and fenchone (9); and retinoic acid (10), respectively. The stereoselective hydroxylation of *gem*-dimethyl on the four-membered ring in mammals was not reported previously.

(1) T. Ishida, Y. Asakawa, T. Takemoto, and T. Aratani, *J. Pharm. Sci.*, **68**, 928 (1979).

(2) G. Germain, P. Main, and M. M. Woolfson, *Acta Crystallogr.*, **B26**, 274 (1970).

(3) A. S. Gupta and S. Dev, *Tetrahedron*, **27**, 635 (1971).

(4) B. M. Lawrence, J. W. Hogg, S. J. Terhune, J. K. Morton, and L. S. Gill, *Phytochemistry*, **11**, 2636 (1972).

(5) R. K. Thappa, V. N. Vashisht, J. Singh, and R. K. Sharma, *Curr. Sci.*, **1970**, 182.

(6) T. Ishida, Y. Asakawa, M. Okano, and T. Aratani, *Tetrahedron Lett.*, **1977**, 2437.

(7) T. Ishida, Y. Asakawa, T. Takemoto, and T. Aratani, *J. Pharm. Sci.*, **70**, 406 (1981).

(8) Y. Asahina and M. Ishidate, *Ber. Dtsch. Chem. Ges.*, **68B**, 947 (1935).

(9) M. Miyazawa, H. Kameoka, K. Morinaga, K. Negoro, and N. Mura, "The Abstracts of 24th Symposium on the Chemistry of Terpenes, Essential Oils and Aromatics," Chemical Society of Japan, Tokyo, Japan, 1980, p. 62 (in Japanese).

(10) R. Hanni, F. Bigler, W. Meister, and G. Fungert, *Helv. Chim. Acta*, **59**, 2221 (1976).

[2] Syntex R3.

Y. Asakawa
Z. Taira
T. Takemoto
Institute of Pharmacognosy
Tokushima Bunri University
Tokushima 770, Japan
T. Ishida ˣ
Hiroshima Institute of Technology
Itsukaichi
Hiroshima 738, Japan
M. Kido
Y. Ichikawa
Laboratories of Natural Products Chemistry
Otsuka Pharmaceutical Co. Ltd.
Kawauchi-cho
Tokushima 771-01, Japan

Received January 12, 1981.
Accepted for publication February 19, 1981.

Relationship between Flow Rates of Granular Powders through Stationary and Moving Orifices

Keyphrases □ Powders, granular—relationship between flow rates of granular powders through stationary and moving orifices □ Flow rates—of powder granulations, prediction of dynamic flow rate from static flow measurements □ Models, mathematical—prediction of dynamic flow rates of powder granulations from static flow measurements

To the Editor:

Since the compressed tablet is the most common dosage form manufactured, the ability to predict scale-up properties of tablet formulations for high-speed processing is needed. To manufacture tablets on a rotary tablet machine, flow of granular material through a stationary orifice (*i.e.*, efflux tube on the granulation hopper) followed by flow into moving orifices (*i.e.*, tablet dies) is required. Since little data have been reported (1, 2) that characterize the latter process of dynamic flow, data from static flow measurements have been used to predict dynamic flow properties of solids. Takieddin *et al.* (3) reported that dynamic flow rates were not predicted successfully from measurements of solid flow through a stationary orifice (static flow), noting that an apparatus suitable for the study of dynamic flow was not available.

An apparatus was constructed to study the dynamic flow of granular materials (4, 5). Although the instrument does not provide an exact duplication of events that occur within the feed frame of a tablet machine, it provides a reasonable means to obtain dynamic flow data. A slight modification of the apparatus also provides a means to study static flow rates.

Dynamic flow measurements of a lactose–cornstarch wet granulation (6) were reported (7). Six measurements were obtained for each combination of granulation mesh cut (20–40, 40–60, and 60–80), orifice size [3/16 (0.48), 1/4 (0.63), 5/16 (0.8), 3/8 (0.95), and 1/2 (1.3) in. (cm)], and five die ve-

0022-3549/81/0600-0711$01.00/0

Table I—Static and Dynamic Flow Rates for Three Granulation Mesh Cuts

Mesh Cut[a] of USP Sieves	Average Particle Diameter[b], cm	Orifice Diameter, in. (cm)	Static Flow Rate (W_s), g/sec	Dynamic Flow Rate (W_2)[c], g/sec
20–40	0.0630	3/16 (0.48)	0.74	0.53
		1/4 (0.63)	1.71	1.24
		5/16 (0.8)	3.11	2.74
		3/8 (0.95)	5.65	4.75
		1/2 (1.3)	12.7	12.4
40–60	0.0335	3/16 (0.48)	1.13	0.88
		1/4 (0.63)	2.43	1.99
		5/16 (0.8)	4.25	3.97
		3/8 (0.95)	7.44	7.02
		1/2 (1.3)	15.5	17.1
60–80	0.0214	3/16 (0.48)	1.31	1.07
		1/4 (0.63)	2.73	2.34
		5/16 (0.8)	4.45	4.48
		3/8 (0.95)	8.19	7.84
		1/2 (1.3)	14.7	18.3

[a] Particle density measurements (5) for the three mesh cuts are: 20–40, ρ = 1.45 g/ml; 40–60, ρ = 1.49 g/ml; and 60–80, ρ = 1.52 g/ml. [b] Average particle diameter is defined as the arithmetic mean of the sieve openings for each pair of USP sieves; this value is an approximation (12). [c] Values of dynamic flow rates reported by Carstensen and Laughlin (7) were incorrect.

locities (between 3 and 12.5 cm/sec); average dynamic flow rates (W_2), as defined by Carstensen and Laughlin (7), are listed in Table I. For static flow measurements, the movable slide of the apparatus was stationary; an aluminum tube (2.54 cm i.d.) centered above the die held the granular material. Measurement of static flow rates was made with the same three granulation mesh cuts and the same five orifice sizes as used during dynamic flow studies. Five measurements with each combination of orifice and particle size were made; mean data are reported as static flow rates (W_s) in Table I. An apparent difference is noted between pairs of values for each set of experimental conditions; the dynamic flow rate is smaller in most cases.

Equations developed for modeling static flow often are based on the Brown–Richards equation (8) and are written in the following form:

$$W_s = f(d)P^{n(d)} \qquad \text{(Eq. 1)}$$

where f and n denote "function of" and n is generally 2.5, a constant. However, n also has been shown to be a function of particle diameter d (9, 10).

Ahmad and Pilpel (9) studied the static flow properties of six different materials. Their mathematical model was based on the Brown–Richards equation and contained a bulk density term and a particle-shape factor term. They reported (9) that one equation could predict the static flow of all six materials with an overall accuracy of ~±7%.

Danish and Parrott (10) studied the static flow properties of a crystalline solid and a granular material and derived separate equations to describe the static flow rate of each material. The Brown–Richards equation was the basis for the derivations; a true density term was included but no particle-shape factor term. They reported a 10% variation between experimental and calculated values for each of the two models.

The Brown–Richards equation can be used to describe static flow for situations where: (*a*) the flow rate decreases as the particle size is increased, (*b*) the orifice size is at least six times greater than the particle size, (*c*) the granulation height is at least two times greater than the orifice diameter, and (*d*) the ratio of orifice diameter to granulation hopper diameter is <0.5. Therefore, it should be possible to write an equation in the form of Eq. 1 that can describe the static flow data shown in Table I. Such an equation, which describes static flow as a function of orifice size (P), particle diameter (d), acceleration due to gravity (g), and particle density[1] (ρ), has been derived; measurements of static flow through the largest orifice were excluded since they failed to meet the fourth criterion for applicability of the Brown–Richards equation. The derivation approach suggested by Danish and Parrott (10) was used (5) and resulted in:

$$W_s = \frac{\pi\rho\sqrt{g}}{4}\left(\frac{P}{1.65 + 2.34d}\right)^{\left(\frac{1}{0.24-0.038\ln d}\right)} \qquad \text{(Eq. 2)}$$

The flow rates predicted with Eq. 2 were larger than the experimentally measured values in eight of 12 cases; the average of the differences between calculated and experimental values (expressed as a percent of experimental data) for static flow was +3.5%.

Dynamic flow rate is not a function of orifice velocity (5). This fact can be concluded from study of Fig. 3 and Eq. 7 in Ref. 7; values for W_2 are calculated from the intercept of each line. Thus, each dynamic flow rate is related to the orifice size and particle diameter but is independent of the orifice velocity. These relationships suggest that dynamic flow also can be expressed in the form of the Brown–Richards equation. Measurements of dynamic flow through the largest orifice were excluded since they apparently failed to meet the first criteria for applicability of the Brown–Richards equation. Previous work indicated that, for dynamic flow, if the exponent n is a constant, it should have a value of 2.9–3.4. Dynamic flow data, collected using the four smallest orifice sizes, were used to derive:

$$W_2 = \frac{\pi\rho\sqrt{g}}{4}\left(\frac{P + 0.0009d^{-1.25}}{2.11 + 0.12\ln d}\right)^{3.33} \qquad \text{(Eq. 3)}$$

The flow rates predicted with Eq. 3 were larger than experimentally measured values in eight of 12 cases. The average of the differences between calculated and experimental values (expressed as a percent of experimental data) for dynamic flow rates was +1.4%.

[1] Brown and Richards (11) reported that it is inappropriate to relate static flow rate to bulk density of the solid material, because bulk density is a combined measurement of the true or particle density and the packing characteristics of the material. They noted that W_s is a function of the voidage at the orifice; this voidage is related to the true density of a crystalline material or to the particle density of a granular material. Since the particle densities of the three granulation mesh cuts are different, it seemed most appropriate to include particle density as the parameter in the equations.

A second equation for prediction of dynamic flow rates was developed, similar in form to Eq. 2 for static flow:

$$W_2 = \frac{\pi\rho\sqrt{g}}{4}\left(\frac{P}{1.52 + 4.12d}\right)^{(2.79+6.68d)} \quad \text{(Eq. 4)}$$

Again, measurements of dynamic flow through the largest orifice were excluded. Now, the exponent n is a function of the particle diameter. The flow rates predicted with Eq. 4 were larger than experimentally measured values in five of 12 cases. The average of the differences between calculated and experimental values (expressed as a percent of experimental data) for dynamic flow rates was −0.4%.

In Eqs. 2–4, which are based on the Brown–Richards equation, the static and dynamic flow rates are expressed in terms of orifice diameter, particle diameter, and particle density. If static and dynamic flow rates are not dependent on any dimensions of the apparatus except the orifice size, it should be possible to combine the relationships. Then dynamic flow rate can be expressed as a function of static flow. If Eqs. 2 and 3 are combined, dynamic flow rates can be predicted using:

$$W_2 = \frac{\pi\rho\sqrt{g}}{4}\left[\left(\frac{1.65 + 2.34d}{2.11 + 0.12\ln d}\right)\left(\frac{4W_s}{\pi\rho\sqrt{g}}\right)^{(0.24-0.038\ln d)} + \left(\frac{0.0009d^{-1.25}}{2.11 + 0.12\ln d}\right)\right]^{3.33} \quad \text{(Eq. 5)}$$

If the predicting power of Eq. 5 is good:

1. There should be the same number of positive and negative differences between calculated and experimental values (+5 and −7).
2. The average of the differences (expressed as a percent of experimental data) should be close to zero (−1.2%).
3. The arithmetic mean of the absolute value of these differences should be small (6.0%).

Thus, Eq. 5 appears to be appropriate for predicting dynamic flow rates for the granular material studied.

When Eqs. 2 and 4 are combined, another algebraic expression is obtained that describes dynamic flow rate as a function of static flow:

$$W_2 = \frac{\pi\rho\sqrt{g}}{4}\left(\frac{1.65 + 2.34d}{1.52 + 4.12d}\right)^{(2.79+6.68d)} \times \left(\frac{4W_s}{\pi\rho\sqrt{g}}\right)^{(0.67+1.60d-0.11\ln d-0.25d\ln d)} \quad \text{(Eq. 6)}$$

If the predicting power of Eq. 6 is good:

1. There should be the same number of positive and negative differences between calculated and experimental values (+0 and −12).
2. The average of the differences (expressed as a percent of experimental data) should be close to zero (−6.2%).
3. The arithmetic mean of the absolute value of these differences should be small (6.2%).

Thus, Eq. 6 appears to have fair predicting power for dynamic flow rates of the granular materials studied, although it is somewhat less accurate than Eq. 5. The limited amount of data precludes selection of the more appropriate general form for an equation to predict dynamic flow rates from static flow data.

The form of Eqs. 2–4 for static and dynamic flow is comparable to equations reported by other investigators (9, 10). While Eqs. 5 and 6 are more cumbersome, they also are of a similar form; the orifice diameter (P) was written implicitly as a function of the static flow rate (W_s). An important observation of Eqs. 5 and 6 is that dynamic flow is not first order in static flow (W_s) if the exponents on the $(4W_s/\pi\rho\sqrt{g})$ term are different than unity. In Eq. 5, the exponent $[(0.24 - 0.038\ln d)\ (3.33)]$ is greater than unity for all d values of <0.21 cm. Similarly, for Eq. 6, the exponent $(0.67 + 1.60d - 0.11\ln d - 0.25d\ln d)$ has a value greater than 1 for all particles sizes (d) of <598 cm. Therefore, for particle sizes commonly found in tablet formulations, both equations predict that the dynamic flow is not first order in static flow. In addition, the dynamic flow is nonlinear with respect to both preexponential terms, which are related indirectly (*i.e.*, through particle density) or directly to the particle diameter.

The direct applicability of Eqs. 5 and 6 to other granulations and dynamic flow systems is questionable. However, the form of the equations explains why the dynamic flow rates are not easily predicted from static flow data. The relationships also suggest that static and dynamic flow rates are dependent on many of the same measurable parameters; these parameters should be considered in the development of other mathematical models for dynamic flow rates.

(1) J. Oakley, *J. Inst. Met.*, **87**, 26 (1958).
(2) J. A. Hersey, *Rheol. Acta*, **4**, 235 (1965).
(3) M. Takieddin, F. Puisieux, J. R. Didry, P. Touré, and D. Duchêne, presented at the First International Conference on Pharmaceutical Technology, Paris, France, 1977.
(4) S. M. Laughlin, L. VanCampen, M. Takieddin, D. Duchêne, F. Puisieux, and J. T. Carstensen, *Int. J. Pharm.*, **3**, 33 (1979).
(5) S. M. Laughlin, M.S. thesis, School of Pharmacy, University of Wisconsin, Madison, Wis., 1979.
(6) J. T. Carstensen, "Pharmaceutics of Solids and Solid Dosage Forms," Wiley–Interscience, New York, N.Y., 1977, p. 210.
(7) J. T. Carstensen and S. M. Laughlin, *Powder Technol.*, **23**, 79 (1979).
(8) R. L. Brown and J. C. Richards, *Trans. Inst. Chem. Eng.*, **38**, 243 (1960).
(9) M. Ahmad and N. Pilpel, *Rheol. Acta*, **8**, 448 (1969).
(10) F. Q. Danish and E. L. Parrott, *J. Pharm. Sci.*, **60**, 548 (1971).
(11) R. L. Brown and J. C. Richards, *Trans. Inst. Chem. Eng.*, **37**, 108 (1959).
(12) D. Brooke, *J. Pharm. Sci.*, **64**, 1409 (1975).

Sharon M. Laughlin ˣ
Jens T. Carstensen
School of Pharmacy
University of Wisconsin
Madison, WI 53706

Received January 28, 1980.
Accepted for publication March 9, 1981.

Mesophase Formation during *In Vitro* Cholesterol Gallstone Dissolution: A Specific Effect of Ursodeoxycholic Acid

Keyphrases □ Cholesterol—gallstones, mesophase formation during *in vitro* gallstone dissolution □ Gallstones, cholesterol—effect of bile acid on gallstone dissolution *in vitro* □ Ursodeoxycholic acid—effect on cholesterol gallstone dissolution *in vitro*, compared with chenodeoxycholic acid □ Dissolution—cholesterol gallstones, effect of bile acid

To the Editor:

Ursodeoxycholate (I), the 7β-epimer of chenodeoxycholate (II), has been shown to be equal or superior to II when used as oral medication for the dissolution of cho-